Biochimica et Biophysica Acta 1818 (2012) 474–480

Contents lists available at SciVerse ScienceDirect

Biochimica et Biophysica Acta

journal homepage: www.elsevier.com/locate/bbamem

Structure–activity relationship of sphingomyelin analogs with sphingomyelinase from *Bacillus cereus*

Christian Sergelius [a], Sanna Niinivehmas [b], Terhi Maula [a], Mayuko Kurita [c], Shou Yamaguchi [c], Tetsuya Yamamoto [c], Shigeo Katsumura [c], Olli T. Pentikäinen [b], J. Peter Slotte [a,*]

[a] *Biochemistry, Department of Biosciences, Åbo Akademi University, Turku, Finland*
[b] *Department of Biological and Environmental Science, P.O. Box 35, FI-40014 University of Jyväskylä, Finland*
[c] *School of Science & Technology, Kwansei Gakuin University, 2-1 Gakuen, Sanda City, Hyogo 669-1337, Japan*

ARTICLE INFO

Article history:
Received 7 September 2011
Received in revised form 11 October 2011
Accepted 17 October 2011
Available online 25 October 2011

Keywords:
3O-methylated sphingomyelin
2N-methylated sphingomyelin
Head group methyl analog
Phytosphingomyelin

ABSTRACT

The aim of this study was to examine how structural properties of different sphingomyelin (SM) analogs affected their substrate properties with sphingomyelinase (SMase) from *Bacillus cereus*. Using molecular docking and dynamics simulations (for SMase–SM complex), we then attempted to explain the relationship between SM structure and enzyme activity. With both micellar and monolayer substrates, 3O-methylated SM was found not to be degraded by the SMase. 2N-methylated SM was a substrate, but was degraded at about half the rate of its 2NH–SM control. PhytoPSM was readily hydrolyzed by the enzyme. PSM lacking one methyl in the phosphocholine head group was a good substrate, but PSM lacking two or three methyls failed to act as substrates for SMase. Based on literature data, and our docking and MD simulations, we conclude that the 3O-methylated PSM fails to interact with Mg^{2+} and Glu53 in the active site, thus preventing hydrolysis. Methylation of 2NH was not crucial for binding to the active site, but appeared to interfere with an induced fit activation of the SMase via interaction with Asp156. An OH on carbon 4 in the long-chain base of phytoPSM appeared not to interfere with the 3OH interacting with Mg^{2+} and Glu53 in the active site, and thus did not interfere with catalysis. Removing two or three methyls from the PSM head group apparently increased the positive charge on the terminal *N* significantly, which most likely led to ionic interactions with Glu250 and Glu155 adjacent to the active site. This likely interaction could have misaligned the SM substrate and hindered proper catalysis.

1. Introduction

Sphingomyelin (SM) is a major constituent in the outer leaflet of many cell membranes [1–3]. It has been argued that SM and other sphingolipids, together with cholesterol, form lateral ordered domains (i.e., lipid rafts) in membranes, which are believed to be important sites for protein–protein interactions [4–7]. The molecular structure of SMs dramatically affects how they interact with other lipids and function in domain formation and thus how they facilitate protein interactions in membranes [8–14].

SM is synthesized from ceramide and phosphatidylcholine (PC), by transfer of the PC head group to ceramide [15]. This transfer is catalyzed by SM synthases 1 or 2, and occurs in the Golgi (synthases 1 and 2) and in the plasma membrane (synthase 2) [16–18]. Ceramides, on the other hand, are formed in the endoplasmic reticulum from a long-chain base and a fatty acid [19], and their transfer to Golgi is mediated by CERT, a ceramide transfer protein [20–22].

SM can be hydrolyzed to ceramide by at least three different classes of sphingomyelinase (SMase) enzymes. The acid SMase is mainly responsible for lysosomal degradation of SM [23], whereas a group of neutral SMases appear to regulate SM levels in cell membranes, in the Golgi, and in mitochondria [24,25]. An alkaline SMase, secreted from intestinal cells, appears to be centrally involved in SM metabolism in the gastrointestinal tract [26].

During the early days of SMase purification from various tissues and microorganisms it was observed that the enzymes were rather specific for SM as substrate, and hydrolyzed e.g., PC very slowly or not at all [27,28]. The effects of substrate modifications on SMase activity have been examined to some extent before. Bittman and coworkers showed with a rat brain neutral SMase that modification of the 3OH in SM with a methyl group, or elimination of the 3OH

Abbreviations: CPE, *N*-palmitoyl-D-*erythro*-sphingosylphosphorylethanolamine; CPE-Me_1, *N*-palmitoyl-D-*erythro*-sphingosylphosphorylethanol-*N*-monomethylamine; CPE-Me_2, *N*-palmitoyl-D-*erythro*-sphingosylphosphorylethanol-*N*,*N*-dimethylamine; CPE-Me_3, *N*-palmitoyl-D-*erythro*-sphingosylphosphorylethanol-*N*,*N*,*N*-trimethylamine (i.e., PSM); MD, molecular dynamics; NMePSM, *N*-palmitoyl-D-*erythro*-2NMe-sphingomyelin; OMePSM, *N*-palmitoyl-D-*erythro*-3OMe-sphingomyelin; PSM, *N*-palmitoyl-D-*erythro*-sphingomyelin; PC, phosphatidylcholine; PhytoPSM, *N*-palmitoyl-D-*erythro*-phytosphingomyelin; SM, sphingomyelin; SMase, sphingomyelinase.

* Corresponding author. Tel.: +358 40 5816521; fax: +358 2 2410014.
E-mail address: jpslotte@abo.fi (J.P. Slotte).

0005-2736/$ – see front matter © 2011 Elsevier B.V. All rights reserved.
doi:10.1016/j.bbamem.2011.10.013

completely prevented enzyme-catalyzed hydrolysis [29]. An SM analog in which the phosphocholine head group was linked to the ceramide 1-OH by a sulfur atom instead of an oxygen was, however, found to be a substrate for SMase from *Bacillus cereus* [30]. In addition, synthesis of various SM analogs has been accomplished in search for SMase inhibitors [31–33].

Chemical modification studies with the SMase from *B. cereus* early suggested that aspartic and glutamic acids are involved in the catalytic and adsorptive activities of the enzyme [34]. Further mutagenesis studies of selected conserved residues in the apparent catalytic site of SMase from *B. cereus* further revealed their importance for retaining full enzyme activity for SM hydrolysis [35,36]. Although many of the human SMase enzymes have been cloned and the genes sequenced, crystallographic structures currently exist only for two SMase enzymes, one for *Listeria ivanovii* [37], and one for *B. cereus* [38]. The accomplishment of structure determination of the *B. cereus* SMase made it possible to better understand the role of conserved amino acid residues for metal ion binding, substrate binding, and catalysis [38]. Recently, the alkaline SMase was homology modeled according to the crystal structure of a nucleotide pyrophosphate/phosphodiesterase from *Xhantomona saxonopodis* [39]. However, the alkaline SMase shares no sequence homology to other SMases.

We have in this study analyzed the catalytic activity of SMase from *B. cereus*, and examined how variation in SM structure (for structures of molecules used, see Scheme 1) affected hydrolysis rates, and how the enzyme activity for a specific substrate molecule could be understood in relation to a molecular fit of the substrate to the substrate binding site of the enzyme. Enzyme activities were measured both with micellar and monolayer substrate, and the substrate binding into the crystal structure of *B. cereus* SMase [38] was examined by employing docking and MD simulations.

2. Materials and methods

2.1. Materials

The substrate sphingolipids were prepared either by the Slotte Laboratory (palmitoyl SM, phytoPSM) or by the Katsumura Laboratory (all other SM analogs used). PSM was purified from egg SM (Avanti Polar Lipids, Alabaster, AL, USA) as described previously [13]. PhytoPSM was prepared from (2S, 3S, 4R)-2-amino-1,3,4-octadecanetriol-1-phosphocholine (Avanti Polar Lipids) by linking palmitoyl anhydride (Sigma-Aldrich, St. Louis, MO, USA) to the free NH_2 group, as described previously [13,40]. The phytoPSM was purified using preparative reverse-phase HPLC chromatography [13] and identified using ESI-MS [13]. NMePSM and OMePSM were prepared as described in [10]. PSM analogs with modified head-group structure (CPE-Me_3, CPE-Me_2, CPE-Me_1, CPE) were prepared as described previously [8]. SMase from *B. cereus* was obtained from Sigma-Aldrich. Water was used as aqueous solvent in all studies. All other inorganic and organic

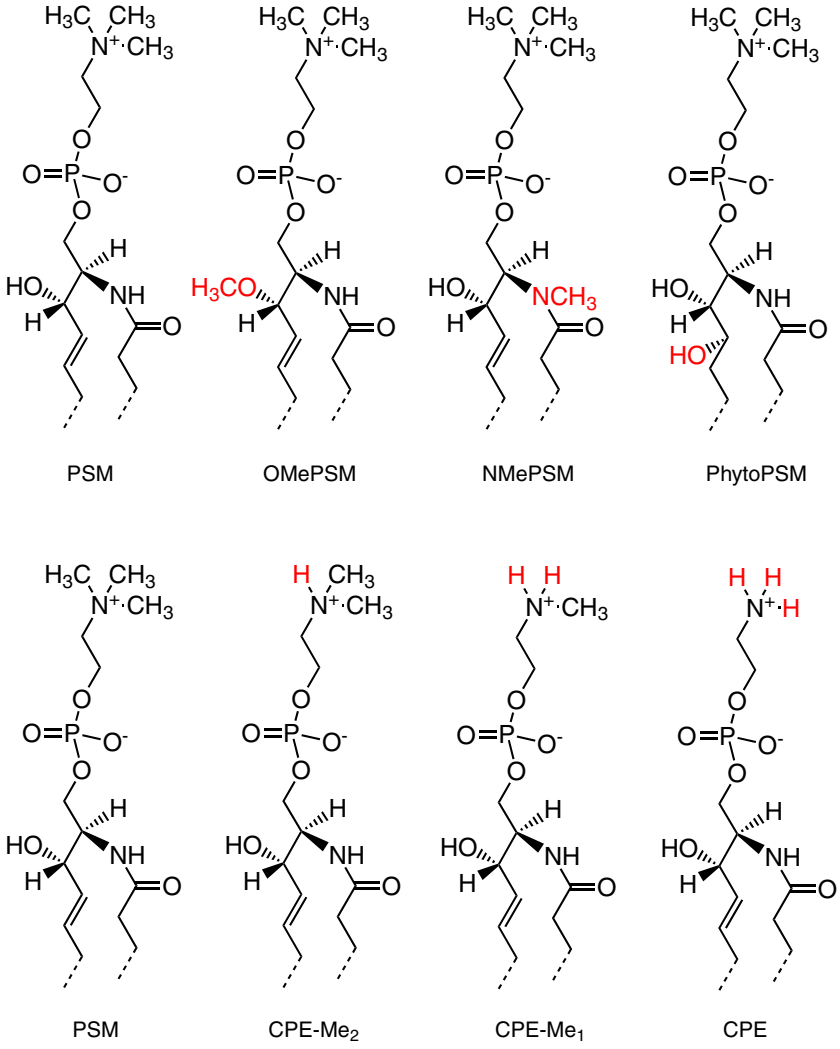

Scheme 1. Chemical structures of the SM analogs used in the study. The upper row shows methylated SM analogs, and below them head group SM analogs are shown.

chemicals used were of the highest purity available. The solvents used were of spectroscopic grade. Water was purified by reverse osmosis followed by passage through a Millipore UF Plus water purification system having final resistivity of 18.2 MΩ cm.

2.2. SMase assay with micellar substrate

To measure substrate properties of SM analogs as micellar substrates, the Amplex® Red Sphingomyelinase Assay Kit (Invitrogen/Molecular Probes, Eugene, OR, USA) was used. The SM micellar solution was prepared in 0.2 wt.% Triton X-100 (detergent supplied in the kit) and subjected to intermittent vortex mixing during a period of 30 min. The substrate micelles had an average diameter of 11 ± 1 nm, and the size was similar for each of the SM analogs. The final concentrations of reactants in the reaction mix were 35.7 μM SM substrate, 5.7 mU/ml of SMase (none in the blank), 14 μM Amplex Red reagent, 286 mU/ml of peroxidase, 28.6 mU/ml of choline oxidase, and 1.14 U/ml of alkaline phosphatase. Substrate and co-enzymes were tempered to 37 °C before starting the reaction by addition of SMase. Excitation/emission was at 560/590 nm, respectively.

2.3. SMase assay with monolayer substrate

To test for SMase substrate properties of SM analogs in monolayer membranes, a previously published method was used [41]. Since the interfacial molecular area of SM and its corresponding ceramide is different (the ceramide being smaller), degradation of SM substrate in a monolayer at constant lateral surface pressure will lead to a monolayer area reduction that is proportional to the amount of SM degraded per time unit. Briefly, the SM analog (in hexane/2-propanol 3:2 vol) was spread on phosphate-buffered saline (pH 7.4), and after a 5 min waiting period, the monolayer was compressed to a surface pressure of 15 mN/m using a KSV 3000 surface barostat (KSV Instruments, Helsinki, Finland). The trough was of a zero-order type with a reaction chamber and a lipid reservoir. During hydrolysis, the reaction chamber contained buffer supplemented with 5 mM $MgCl_2$ and 0.3 U of SMase in a volume of about 30 ml. The surface pressure was maintained at 20 mN/m during the course of the reaction.

2.4. Computational studies

The structure of PSM was sketched with SYBYL7.3 (Tripos, St. Louis, MO, USA), and minimized using a conjugate gradient method (max iterations 100,000) with MMFF94s charges [42] and a dielectric constant of 10.

The 3D structure of *B. cereus* SMase (PDB: 2DDR [38]) was acquired from the Protein Data Bank [43]. Peptide chain C of 2DDR was chosen because it contains structural data for the complete amino acid sequence. Calcium ions seen in the crystal structure were replaced with magnesium ions because magnesium ions were used as cations in the experimental setup. TLEAP in ANTECHAMBER 1.27 [44] was used to add hydrogen atoms into the protein structure.

The docking of PSM was performed flexibly with GOLD 5.0 [45] using GoldScore scoring function and the most accurate (slow) option.

The docking conformation of PSM for MD simulation was selected based on the close proximity of catalytic His296 to the reaction center (phosphorus).

TLEAP in ANTECHAMBER 1.27 was used to create force field parameters for the protein (ff03) [46] and the ligand (gaff) [47]. The protein–ligand complex was solvated with a rectangular box of transferable intermolecular potential three-point water molecules [48] extending 13 Å in all directions from the sides of the protein. Energy minimizations and MD simulations were performed with NAMD 2.6 [49].

The protein–ligand complex was equilibrated in three steps. First, water molecules and amino acid side chains were minimized with a conjugate gradient algorithm, while the rest of the system was kept in place with the harmonic force of 5 kcal mol^{-1} $Å^{-2}$. In the second minimization step ligand–protein complex and water molecules were minimized without constraints. As a third step, an MD simulation was run for 360 ps with 2.0 fs time-step at constant temperature (300 K) and pressure (1 atm). Water molecules and amino acid side chains were allowed to move, while the rest of the system was restrained as in the first energy minimization step. Finally, the equilibrated protein–ligand complex was simulated for 7.2 ns with 1.0 fs time-step at constant temperature (300 K) and at constant pressure (1 atm) with the Langevin Piston method. In MD simulations a cut-off value of 12 Å was used for van der Waals interactions and electrostatics were treated with the Particle Mesh Ewald (PME) method [50]. The simulations were performed under periodic boundary conditions. Figs. 3 and 4 were prepared using BODIL [51], MOLSCRIPT v 2.1.2 [52], and the RASTER3D package [53].

3. Results

3.1. Micellar substrate properties of various SM analogs

Using the Amplex® Red Sphingomyelinase Assay Kit we were able to assess the substrate properties of various SM analogs that had phosphocholine in their head group. We complemented the kit by using SMase from *B. cereus* as the source of the SM hydrolytic activity. The *B. cereus* enzyme was used since its 3D structure is known [38]. The Amplex® Red reaction only gives relative information about enzyme activity, and hence it was important to compare different substrate analogs using as similar as possible reaction conditions. After a lag phase of 6–11 min, the reaction appeared to be linear with time (at least during the first 30 min — Fig. 1). When comparing NMePSM and OMePSM analogs with PSM, it was evident that whereas NMePSM was a substrate, OMePSM was not. The slope of the change in fluorescence intensity over time was about 54% for NMePSM (when the PSM slope was set to 100%). The slope for OMePSM was about 1% (Fig. 1). Previously, it was shown that an OMeSM analog was not a substrate for neutral SMase from rat brain [29]. It was further stated that the OMeSM analog actually behaved as an inhibitor of neutral SMase from rat brain (IC_{50} value about 50 μM — [29]). PhytoSM, which has an additional hydroxyl on carbon 4 in the long-chain base, was a good substrate for the SMase from *B. cereus* (Fig. 1).

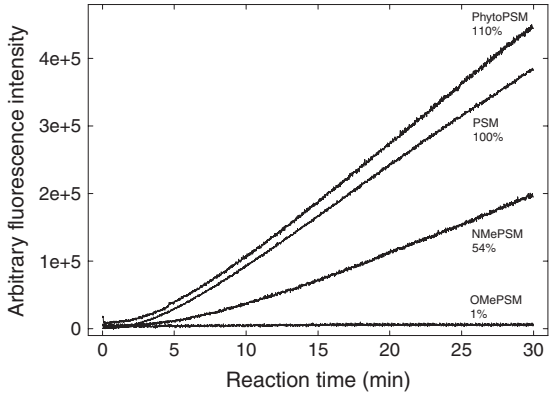

Fig. 1. Hydrolysis of SM analogs prepared as micellar substrates by SMase from *Bacillus cereus* at 37 °C. The fluorescence assay is described in detail under Materials and methods. Each sample contained 100 nmol of SM analog, and the reaction was started by injecting the substrate at time zero. The reaction was followed during 30 min, and the slope for the last 10 min was calculated by linear regression. The slope for PSM was set to 100%, and the other slopes are relative to this. Representative curves are shown.

To test for the inhibitory efficacy of OMePSM, we measured the rate of PSM hydrolysis in the presence or absence of OMePSM. Substrate preparations were made to either include OMePSM in the PSM micelles (equimolar ratio), or to add OMePSM in separate micelles to the reaction mix (again to an equimolar ratio). The hydrolysis of PSM was only marginally affected by the presence of equimolar amounts of OMePSM in the reaction mix (Fig. 2). Both the slope and the total fluorescence at 30 min were slightly less when PSM and OMePSM were in the same micelles, as compared to the situation in which PSM and OMePSM were in separate micelles. It appears that binding of OMePSM to the active site of SMase from *B. cereus* is not very stable and is fully reversible. Therefore, based on our results, we do not consider OMePSM to be a potent inhibitor of SMase from *B. cereus*.

3.2. Docking of PSM to the active site of SMase from B. cereus

To better understand the substrate properties of some SM analogs, we docked PSM to the active site of SMase and deduced from the docking and from MD simulations how substrate structure relates to substrate properties. Both docking and MD simulations suggest that the 3OH group of PSM coordinates to the magnesium ion, and simultaneously donates a hydrogen bond to the carboxylate group of Glu53 (Fig. 3). Also, we observed that the carbonyl oxygen atom of PSM accepted a hydrogen bond from Lys131. The docking simulation did not predict interactions with the 2NH group of PSM. However, during the MD simulation the nearby loops (Val118–Gly132 and Thr150–Pro164) adjusted to closer proximity of 2NH. As a result, an induced fit mechanism (Fig. 4) during the substrate binding appeared to pull up Asp156 to form a hydrogen bond with 2NH of PSM (Fig. 3). Both the long-chain base and the *N*-linked acyl chain of PSM extended into two directions following the curvature of the protein (Fig. 4).

3.3. Binding of sphingomyelin analogs

Since the 3OH group has a dual role in the binding of substrate to SMase, and since the reaction center is located next to it, it is expected that OMePSM cannot successfully bind into the same position as PSM. Accordingly, SMase fails to degrade OMePSM. Methylation of 2NH is likely to interfere with interactions that PSM has with the side chain of Asp156. The loss of induced fit effect in substrate binding could lead into similar reduction of enzymatic activity as observed earlier for Asp156Gly mutation [35].

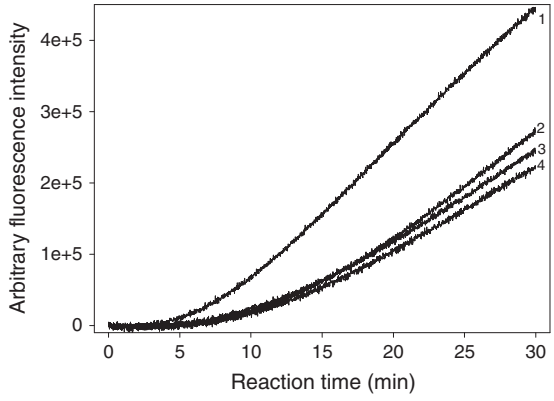

Fig. 2. Hydrolysis of SM analogs prepared as micellar substrates by SMase from *Bacillus cereus* at 37 °C in the presence of potential inhibitor. The fluorescence assay is described in detail under Materials and methods. Each sample contained 100 nmol of SM analog (except line 2 with only 50 nmol PSM). The sample represented by line 3 contains 50 nmol PSM and 50 nmol OMePSM, co-mixed in the same micelles. For line 4, the sample contained 50 nmol PSM in one population of micelles, and 50 nmol OMePSM in another population of micelles. These micelles were admixed at time zero. The reaction was started by adding substrate at time zero, and was followed during 30 min, and the slope for the last 10 min was calculated by linear regression for each sample. The slope for PSM was set to 100%, and the slopes for lines 2, 3 and 4 were about 80%, 68% and 62%, respectively. Representative curves are shown.

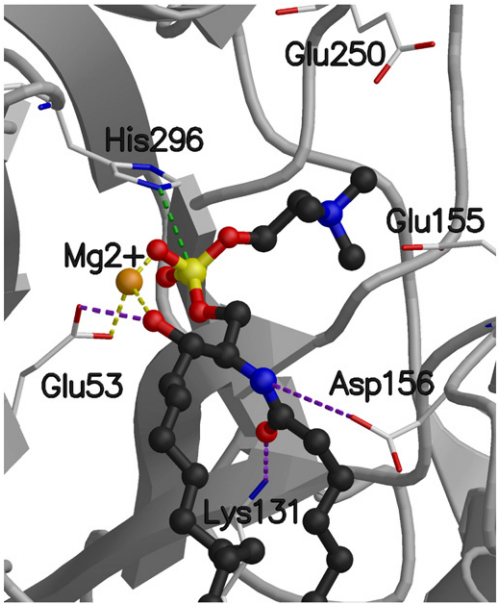

Fig. 3. PSM and its key interactions with SMase from *Bacillus cereus*. PSM was docked into the catalytic site of SMase. The enzyme is shown with secondary structures whereas PSM is shown as ball-and-stick. The 3OH group of PSM coordinates to the magnesium ion and donates a hydrogen bond to the carboxylate group of Glu53. The carbonyl oxygen atom of PSM accepts a hydrogen bond from Lys131. Asp156 forms a hydrogen bond with 2NH of PSM. For reaction, the catalytic His296 is in the close proximity to phosphorus (green dotted line). Hydrogen bonds and metal coordination are shown with purple and yellow dotted lines, respectively.

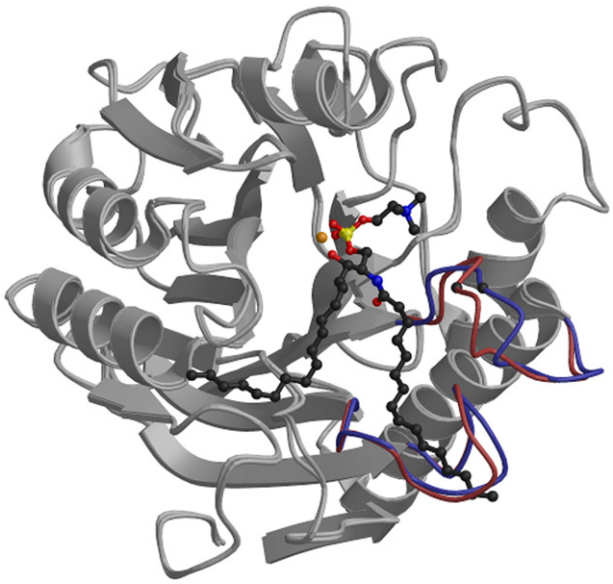

Fig. 4. Induced fit after binding of SM to the active site. MD simulation of the SMase 3D structure after binding of SM to the active site indicate that loops Val118–Gly132 and Thr150–Pro164 shift position. Loops shown in blue represent the position before and loops in red after the MD simulations. The α-carbon of Asp156 is shown in black ball-and-stick. For other simulation conditions, please refer to the Materials and methods section.

3.4. Substrate properties of SM analogs in monolayer membranes

To measure SMase-induced hydrolysis of some head group analogs of SM, the Amplex® Red micellar assay could not be used, since choline oxidase does not recognize other substrates than choline. Instead, we determined relative hydrolysis using a monolayer assay developed in our laboratory [41]. The assay was performed under constant lateral packing density (i.e., constant lateral surface pressure). Hydrolysis results in smaller monolayer area, since the molecular area requirements of ceramides are smaller than their corresponding SM precursors. A typical PSM degradation curve is shown in Fig. 5, in which a small lag phase can be identified, followed by a rapid hydrolysis stage, ending with a condition where substrate availability (and ceramide enrichment) causes the reaction to slow down markedly. NMePSM was a good substrate even for the monolayer assay, but reaction rates were markedly slower when compared to PSM. OMePSM was not a substrate for SMase when presented as a monolayer (data not shown). PhytoPSM appeared to give a slightly longer lag phase compared to PSM, but otherwise the speed of reaction was comparable to that of PSM. The total monolayer area change was smaller for phytoPSM than for PSM, suggesting that the difference in molecular area between ceramide and the precursor SM was smaller for the phytosphingolipid pair when compared to palmitoylceramide and PSM.

In Fig. 6, we show SMase-induced degradation of three head group analogs of PSM, and compare their degradation with that of PSM. When one methyl was removed from the phosphocholine head group (CPE-Me_2), the lag time increased slightly, but the rate of degradation (measured as monolayer area decrease) was fairly similar to that seen with PSM. Clearly, CPE-Me2 was a good substrate for SMase from *B. cereus*, despite the omission of one methyl group from the phosphocholine head group. However, when two or three methyls were removed (CPE-Me_1 and CPE), the substrate properties were lost and no degradation by SMase was evident (Fig. 6).

4. Discussion

In this study we have measured SMase activities for different SM substrates and tried to interpret the SM substrate properties based on substrate docking and MD simulations. The SM substrates were presented to SMase in two different ways: either using mixed micelle substrates in Triton X-100, or using substrates as monolayers at the air/buffer interface. With micellar substrates, the SMase activity determination was based on the oxidation of choline (released as phosphocholine from the SM head group by SMase). Although it is possible that different SM analogs would form different types of mixed micelles with Triton X-100, our finding that all examined mixed SM analog micelles were of similar size (11 ± 1 nm diameter), suggests that major physical differences in the substrate micelles were not directly responsible for the observed differences in catalysis rates. With the monolayer assay, absolute hydrolysis rates are possible to be obtained provided that mean molecular areas of substrate and product are known [41,54]. We did not have this information, and therefore our monolayer results are qualitative and not quantitative.

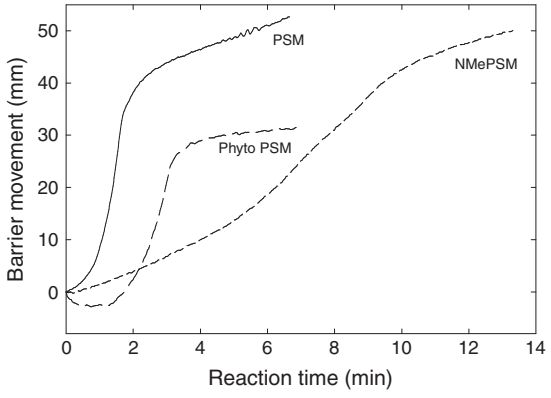

Fig. 5. Hydrolysis of monolayer substrates under constant surface pressure conditions by SMase from *Bacillus cereus* at 37 °C. Monolayers containing one of the SM analogs (PSM, phytoPSM or NMePSM) were prepared at the buffer/air interface, and the monolayer was compressed to a lateral surface pressure of 15 mN/m. At time zero, enzyme was added to the subphase (about 10 mU/ml) of the reaction chamber, and the concomitant reduction of monolayer area was recorded (positive barrier movement).

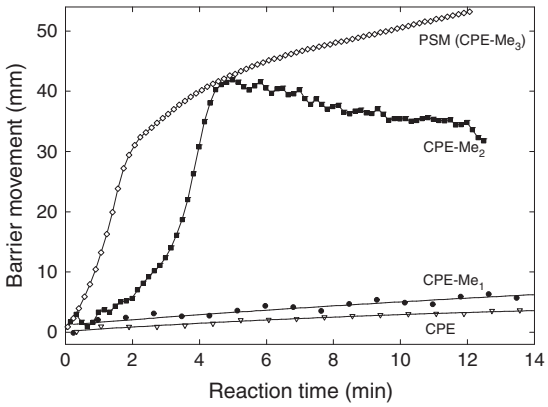

Fig. 6. Hydrolysis of monolayer substrates under constant surface pressure conditions by SMase from *Bacillus cereus* at 37 °C. Monolayers containing one of the head group SM analogs (PSM or CPE-Me_3, CPE-Me_2, CPE-Me_1, and CPE) were prepared at the buffer/air interface, and the monolayer was compressed to a lateral surface pressure of 15 mN/m. At timce zero, enzyme was added to the subphase (about 10 mU/ml) of the reaction chamber, and the concomitant reduction of monolayer area was recorded (positive barrier movement).

The active site of SMase from *B. cereus* is well defined, because of the crystal structure [38], but also because of mutagenesis studies on conserved amino acid residues performed before the structure became available [35,36,55,56]. Glu53 is the essential Mg^{2+} binding amino acid (cation binding site A), whereas His296 is centrally involved in catalysis [38]. The 3OH of the SM substrate is likely to interact both with Mg^{2+} and with Glu53 (Fig. 3 and [38]). In light of these interactions, it is obvious that SMase from *B. cereus* is active only with the natural D-*erythro* SM substrate. Accordingly, it was experimentally shown that both the L-*erythro* [55,57] and the L-*threo* [55] SM analogs are not degraded efficiently by SMases. It is therefore also not surprising that methylation of the 3OH in PSM made the SM analog a non-substrate for SMase from *B. cereus*. Since the 3-OMe analog of SM, as well as the 3-deoxy analog of SM, made these substrates unhydrolyzable with a rat brain neutral SMase [29], it is likely that the active site of that enzyme is similar to the one of *B. cereus*. Indeed, Glu53 and His296 are conserved in the gene for SMase of both *B. cereus* and rat (data not shown).The 3OMe analog of SM was reported to be a low affinity inhibitor of the rat neutral SMase [29]. While this may be the case for the rat enzyme, our interpretation of our own results with the SMase from *B. cereus* is that the 3O-methylated SM analog was mainly a non-substrate and affected the hydrolysis of PSM (when both were present at equimolar ratio) only by diluting the substrate concentration in the mixed micelles (Fig. 2).

Looking further at the active site of *B. cereus* SMase, it is probable that Asp156 and Lys131 stabilized the substrate in the active site by interacting with the 2-NH and the carbonyl oxygen of the *N*-linked acyl chain, respectively (Fig. 3). Methylation of the 2-NH caused the hydrolysis rate to drop by half (micellar assay, Fig. 1) or even more (monolayer assay, Fig. 5). It is evident that proper stabilization of the 2NH and the carbonyl oxygen of the *N*-linked acyl chain were important for maintaining the substrate in a proper location for catalysis to occur efficiently. Supporting evidence for this interpretation has been provided by mutagenesis studies, in which the Asp156 was changed to Gly. This mutation did not render the enzyme inactive, but severely reduced catalysis efficiency when SM was the substrate

[35]. Our MD simulation results further suggest that binding of SM to the active site changes the orientation of loops Val118–Gly132 and Thr150–Pro164 so that the interaction between Asp156 and the 2NH of SM becomes more pronounced (Fig. 4). This induced fit is likely to contribute to efficient hydrolysis of a native SM substrate.

Although phytoSM is not a major SM species, other sphingolipids containing the phyto long-chain base are more common [58–61]. However, we synthesized the phytoPSM analog and tested its substrate properties with the SMase from *B. cereus*. PhytoPSM has an OH-group in the C4 position, in addition to the 3OH group, in the long-chain base. In phytoPSM an internal hydrogen bond might form between the 4OH and 2NH of sphingomyelin or between the 4OH and carbonyl oxygens of the *N*-linked acyl chains. If this hydrogen bond forms, induced fit during the substrate binding does not necessarily occur. However, formation of this hydrogen bond would require twisting of both the phytosphingosine long-chain base and the palmitoyl group of phytoPSM. The alteration of postures of carbon chains takes time, which could lead to prolonged lag-time before the hydrolysis reaction can commence. This was actually the case when phytoPSM was presented to SMase as a monolayer substrate (Fig. 5). A clear difference in lag time between PhytoPSM and PSM was not evident in the Amplex® Red Sphingomyelinase Assay (Fig. 1). However, since this assay is indirect (relying on several helper enzymes before signal is obtained) the lag time information obtained from the monolayer assay is likely to be more reliable.

Next, we analyzed the substrate properties of SM analogs in which the number of terminal methyls on the phosphocholine head group was varied (from three in PSM to zero in ceramide phosphoethanolamine). In the previous study with rat brain neutral SMase, Lister and coworkers also included *N*-demethyl SM (equals our CPE-Me_2) in their assay [29]. They reported that *N*-demethyl SM was not an inhibitor, and was hydrolyzed at a rate one fifth of that seen with SM. We determined that CPE-Me_2 was hydrolyzed at about half the rate of PSM by the SMase from *B. cereus*. Qualitatively our results agree with the study of Lister and coworkers, since CPE-Me_2 was demonstrated to be a substrate. However, rates are difficult to compare, since both the enzyme source and the physical state of the substrate were different. Removing additional methyls from the terminal *N* rendered the SM analogs non-substrates. SM is a zwitterionic phospholipid, which has a partial positive charge on the terminal *N* in the head group, and a partial negative charge on a phosphate oxygen. Removing one, two or all three methyls strengthens the positive charge on the *N*. Apparently, when the positive charge on *N* becomes strong enough, and steric effects of the terminal methyls diminish, a new interaction may form between the *N* of the head group and the Glu250 adjacent to the active site (Fig. 3). Such an interaction could misalign the SM molecule in the active site, especially with regard to Glu53 and Mg^{2+}, and hinder catalysis. We believe this is the likely scenario which could explain why CPE-Me_1 and CPE are non-substrates for SMase.

In conclusion, we have combined enzyme activity measurements with computational studies to better understand how the structure of SM affects its substrate properties for a SMase with a known 3D structure. Proper alignment of the SM substrate to the active site requires a specific orientation of both the 2NH and the 3OH. The proper head group volume and charge also appear to be important for correct alignment of the SM molecule in the active site. It is interesting to note that while SMase from e.g., *B. cereus* has a fairly strict substrate requirement, this is not necessarily the case for all phospholipases. A recent enzyme activity/molecular docking study explored convincingly the molecular reasons for the broad substrate specificity of the α-toxin phospholipase C from *C. perfringens* [62].

Acknowledgements

Valuable comments by Dr. Konstantin Denessiouk is warmly acknowledged. Financial support has been provided by the Sigrid Juselius Foundation (J.P.S.), Åbo Akademi University (J.P.S.), Maa-ja vesitekniikantuki, ry. (O.T.P.), and Grant-in-Aid for Science Research on Priority Areas 16073222 from the Ministry of Education, Culture, Sports, Science and Technology (S.K.) and also the Matching Fund Subsidy for a Private University, Japan (S.K.).

References

[1] Y. Barenholz, T.E. Thompson, Sphingomyelin: biophysical aspects, Chem. Phys. Lipids 102 (1999) 29–34.
[2] B. Ramstedt, J.P. Slotte, Membrane properties of sphingomyelins, FEBS Lett. 531 (2002) 33–37.
[3] J.P. Slotte, Sphingomyelin–cholesterol interactions in biological and model membranes, Chem. Phys. Lipids 102 (1999) 13–27.
[4] A. Pralle, P. Keller, E.L. Florin, K. Simons, J.K. Horber, Sphingolipid–cholesterol rafts diffuse as small entities in the plasma membrane of mammalian cells, J. Cell Biol. 148 (2000) 997–1008.
[5] K. Simons, D. Toomre, Lipid rafts and signal transduction, Nat. Rev. Mol. Cell Biol. 1 (2000) 31–39.
[6] K. Simons, G. van Meer, Lipid sorting in epithelial cells, Biochemistry 27 (1988) 6197–6202.
[7] K. Simons, W.L. Vaz, Model systems, lipid rafts, and cell membranes, Annu. Rev. Biophys. Biomol. Struct. 33 (2004) 269–295.
[8] A. Bjorkbom, T. Rog, K. Kaszuba, M. Kurita, S. Yamaguchi, M. Lonnfors, T.K. Nyholm, I. Vattulainen, S. Katsumura, J.P. Slotte, Effect of sphingomyelin headgroup size on molecular properties and interactions with cholesterol, Biophys. J. 99 (2010) 3300–3308.
[9] A. Bjorkbom, T. Yamamoto, S. Kaji, S. Harada, S. Katsumura, J.P. Slotte, Importance of the phosphocholine linkage on sphingomyelin molecular properties and interactions with cholesterol; a study with phosphate oxygen modified sphingomyelin-analogues, Biochim. Biophys. Acta 1778 (2008) 1501–1507.
[10] A. Bjorkbom, T. Rog, P. Kankaanpaa, D. Lindroos, K. Kaszuba, M. Kurita, S. Yamaguchi, T. Yamamoto, S. Jaikishan, L. Paavolainen, J. Paivarinne, T.K. Nyholm, S. Katsumura, I. Vattulainen, J.P. Slotte, N- and O-methylation of sphingomyelin markedly affects its membrane properties and interactions with cholesterol, Biochim. Biophys. Acta 1808 (2011) 1179–1186.
[11] A. Bjorkbom, B. Ramstedt, J.P. Slotte, Phosphatidylcholine and sphingomyelin containing an elaidoyl fatty acid can form cholesterol-rich lateral domains in bilayer membranes, Biochim. Biophys. Acta 1768 (2007) 1839–1847.
[12] S. Jaikishan, J.P. Slotte, Effect of hydrophobic mismatch and interdigitation on sterol/sphingomyelin interaction in ternary bilayer membranes, Biochim. Biophys. Acta 1808 (2011) 1940–1945.
[13] S. Jaikishan, A. Bjorkbom, J.P. Slotte, Sphingomyelin analogs with branched N-acyl chains: the position of branching dramatically affects acyl chain order and sterol interactions in bilayer membranes, Biochim. Biophys. Acta 1798 (2010) 1987–1994.
[14] B. Ramstedt, J.P. Slotte, Comparison of the biophysical properties of racemic and d-erythro-N- acyl sphingomyelins, Biophys. J. 77 (1999) 1498–1506.
[15] Y. Barenholz, Sphingomyelin–lecithin balance in membranes: composition, structure, and function relationships, in: M. Shinitzky (Ed.), Physiology of Membrane Fluidity, vol. 1, CRC press, Boca Raton, 1984, pp. 131–174.
[16] F.G. Tafesse, K. Huitema, M. Hermansson, S. van der Poel, J. van den Dikkenberg, A. Uphoff, P. Somerharju, J.C. Holthuis, Both sphingomyelin synthases SMS1 and SMS2 are required for sphingomyelin homeostasis and growth in human HeLa cells, J. Biol. Chem. 282 (2007) 17537–17547.
[17] K. Huitema, J. van den Dikkenberg, J.F. Brouwers, J.C. Holthuis, Identification of a family of animal sphingomyelin synthases, EMBO J. 23 (2004) 33–44.
[18] S. Yamaoka, M. Miyaji, T. Kitano, H. Umehara, T. Okazaki, Expression cloning of a human cDNA restoring sphingomyelin synthesis and cell growth in sphingomyelin synthase-defective lymphoid cells, J. Biol. Chem. 279 (2004) 18688–18693.
[19] K. Hirschberg, J. Rodger, A.H. Futerman, The long-chain sphingoid base of sphingolipids is acylated at the cytosolic surface of the endoplasmic reticulum in rat liver, Biochem. J. 290 (1993) 751–757.
[20] K. Hanada, Intracellular trafficking of ceramide by ceramide transfer protein, Proc. Jpn. Acad. Ser. B Phys. Biol. Sci. 86 (2010) 426–437.
[21] K. Hanada, K. Kumagai, N. Tomishige, T. Yamaji, CERT-mediated trafficking of ceramide, Biochim. Biophys. Acta 1791 (2009) 684–691.
[22] K. Hanada, K. Kumagai, S. Yasuda, Y. Miura, M. Kawano, M. Fukasawa, M. Nishijima, Molecular machinery for non-vesicular trafficking of ceramide, Nature 426 (2003) 803–809.
[23] T. Linke, G. Wilkening, S. Lansmann, H. Moczall, O. Bartelsen, J. Weisgerber, K. Sandhoff, Stimulation of acid sphingomyelinase activity by lysosomal lipids and sphingolipid activator proteins, Biol. Chem. 382 (2001) 283–290.
[24] S. Tomiuk, M. Zumbansen, W. Stoffel, Characterization and subcellular localization of murine and human magnesium-dependent neutral sphingomyelinase, J. Biol. Chem. 275 (2000) 5710–5717.
[25] D. Milhas, C.J. Clarke, Y.A. Hannun, Sphingomyelin metabolism at the plasma membrane: implications for bioactive sphingolipids, FEBS Lett. 584 (2010) 1887–1894.
[26] R.D. Duan, L. Nyberg, A. Nilsson, Alkaline sphingomyelinase activity in rat gastrointestinal tract: distribution and characteristics, Biochim. Biophys. Acta 1259 (1995) 49–55.
[27] B.G. Rao, M.W. Spence, Sphingomyelinase activity at pH 7.4 in human brain and a comparison to activity at pH 5.0, J. Lipid Res. 17 (1976) 506–515.

[28] H. Ikezawa, M. Mori, T. Ohyabu, R. Taguchi, Studies on sphingomyelinase of *Bacillus cereus*. I. Purification and properties, Biochim. Biophys. Acta 528 (1978) 247–256.
[29] M.D. Lister, Z.S. Ruan, R. Bittman, Interaction of sphingomyelinase with sphingomyelin analogs modified at the C-1 and C-3 positions of the sphingosine backbone, Biochim. Biophys. Acta 1256 (1995) 25–30.
[30] T. Hakogi, S. Fujii, M. Morita, K. Ikeda, S. Katsumura, Synthesis of sphingomyelin sulfur analogue and its behavior toward sphingomyelinase, Bioorg. Med. Chem. Lett. 15 (2005) 2141–2144.
[31] T. Hakogi, M. Taichi, S. Katsumura, Synthesis of a nitrogen analogue of sphingomyelin as a sphingomyelinase inhibitor, Org. Lett. 5 (2003) 2801–2804.
[32] T. Hakogi, Y. Monden, M. Taichi, S. Iwama, S. Fujii, K. Ikeda, S. Katsumura, Synthesis of sphingomyelin carbon analogues as sphingomyelinase inhibitors, J. Org. Chem. 67 (2002) 4839–4846.
[33] T. Hakogi, Y. Monden, S. Iwama, S. Katsumura, Stereocontrolled synthesis of a sphingomyelin methylene analogue as a sphingomyelinase inhibitor, Org. Lett. 2 (2000) 2627–2629.
[34] M. Tomita, Y. Ueda, H. Tamura, R. Taguchi, H. Ikezawa, The role of acidic amino-acid residues in catalytic and adsorptive sites of *Bacillus cereus* sphingomyelinase, Biochim. Biophys. Acta 1203 (1993) 85–92.
[35] H. Tamura, K. Tameishi, A. Yamada, M. Tomita, Y. Matsuo, K. Nishikawa, H. Ikezawa, Mutation in aspartic acid residues modifies catalytic and haemolytic activities of *Bacillus cereus* sphingomyelinase, Biochem. J. 309 (Pt 3) (1995) 757–764.
[36] H. Ikezawa, K. Tameishi, A. Yamada, H. Tamura, K. Tsukamoto, Y. Matsuo, K. Nishikawa, Studies on the active sites of *Bacillus cereus* sphingomyelinase: substitution of some amino acids by site-directed mutagenesis, Amino Acids 9 (1995) 293–298.
[37] A.E. Openshaw, P.R. Race, H.J. Monzo, J.A. Vazquez-Boland, M.J. Banfield, Crystal structure of SmcL, a bacterial neutral sphingomyelinase C from *Listeria*, J. Biol. Chem. 280 (2005) 35011–35017.
[38] H. Ago, M. Oda, M. Takahashi, H. Tsuge, S. Ochi, N. Katunuma, M. Miyano, J. Sakurai, Structural basis of the sphingomyelin phosphodiesterase activity in neutral sphingomyelinase from *Bacillus cereus*, J. Biol. Chem. 281 (2006) 16157–16167.
[39] J. Duan, J. Wu, Y. Cheng, R.D. Duan, Understanding the molecular activity of alkaline sphingomyelinase (NPP7) by computer modeling, Biochemistry 49 (2010) 9096–9105.
[40] R. Cohen, Y. Barenholz, S. Gatt, A. Dagan, Preparation and characterization of well defined D-*erythro* sphingomyelins, Chem. Phys. Lipids 35 (1984) 371–384.
[41] M. Jungner, H. Ohvo, J.P. Slotte, Interfacial regulation of bacterial sphingomyelinase activity, Biochim. Biophys. Acta 1344 (1997) 230–240.
[42] T. Halgren, Merck molecular force field. I. Basis, form, scope, parameterization, and performance of MMFF94, J. Comput. Chem. 17 (1996) 490–519.
[43] H.M. Berman, J. Westbrook, Z. Feng, G. Gilliland, T.N. Bhat, H. Weissig, I.N. Shindyalov, P.E. Bourne, The protein data bank, Nucleic Acids Res. 28 (2000) 235–242.
[44] J. Wang, W. Wang, P.A. Kollman, D.A. Case, Automatic atom type and bond type perception in molecular mechanical calculations, J. Mol. Graph. Model. 25 (2006) 247–260.
[45] G. Jones, P. Willett, R.C. Glen, Molecular recognition of receptor sites using a genetic algorithm with a description of desolvation, J. Mol. Biol. 245 (1995) 43–53.
[46] Y. Duan, C. Wu, S. Chowdbury, M.C. Lee, G. Xiong, W. Zhang, R. Yang, P. Cieplak, R. Luo, T. Lee, J. Caldwell, J. Wang, P.A. Kollman, A point-charge force field for molecular mechanics simulations of proteins based on condensed-phase quantum mechanical calculations, J. Comput. Chem. 21 (2003) 1999–2012.
[47] J. Wang, R.M. Wolf, J.W. Caldwell, P.A. Kollman, Development and testing of a general AMBER force field, J. Comput. Chem. 25 (2004) 1157–1174.
[48] J. Åqvist, Ion–water interaction potentials derived from free energy perturbation simulations, J. Phys. Chem. B 94 (1990) 8021–8024.
[49] J.C. Phillips, R. Braun, W. Wang, J. Gumbart, E. Tajkhorshid, E. Villa, C. Chipot, R.D. Skeel, L. Kalé, K. Schulten, Scalable molecular dynamics with NAMD, J. Comput. Chem. 26 (2005) 1781–1802.
[50] T. Darden, Y. York, L. Pedersen, An W log(N) method for Ewald sums in large systems, J. Chem. Phys. 98 (1993) 10089–10092.
[51] J.V. Lehtonen, D.J. Still, V.V. Rantanen, J. Ekholm, D. Bjorklund, Z. Iftikhar, M. Huhtala, S. Repo, A. Jussila, J. Jaakkola, O. Pentikainen, T. Nyronen, T. Salminen, M. Gyllenberg, M.S. Johnson, BODIL: a molecular modeling environment for structure–function analysis and drug design, J. Comput. Aided Mol. Des. 18 (2004) 401–419.
[52] P. Kraulis, MOLSCRIPT: a program to produce both detailed and schematic plots of protein structures, J. Appl. Crystallogr. 24 (1991) 946–950.
[53] E.A. Merritt, D.J. Bacon, Raster3D: photorealistic molecular graphics, Meth. Enzymol. 277 (1997) 505–524.
[54] M.L. Fanani, B. Maggio, Kinetic steps for the hydrolysis of sphingomyelin by *Bacillus cereus* sphingomyelinase in lipid monolayers, J. Lipid Res. 41 (2000) 1832–1840.
[55] S. Fujii, K. Ogata, B. Inoue, S. Inoue, M. Murakami, S. Iwama, S. Katsumura, M. Tomita, H. Tamura, K. Tsukamoto, H. Ikezawa, K. Ikeda, Roles of asp126 and asp156 in the enzyme function of sphingomyelinase from *Bacillus cereus*, J. Biochem. 126 (1999) 90–97.
[56] M. Tomita, Y. Ueda, H. Tamura, R. Taguchi, H. Ikezawa, The role of acidic amino-acid residues in catalytic and adsorptive sites of *Bacillus cereus* sphingomyelinase, Biochim. Biophys. Acta 1203 (1993) 85–92.
[57] Y. Barenholz, A. Roitman, S. Gatt, Enzymatic hydrolysis of sphingolipids. II. Hydrolysis of sphingomyelin by an enzyme from rat brain, J. Biol. Chem. 241 (1966) 3731–3737.
[58] Y. Mizutani, A. Kihara, Y. Igarashi, Identification of the human sphingolipid C4-hydroxylase, hDES2, and its up-regulation during keratinocyte differentiation, FEBS Lett. 563 (2004) 93–97.
[59] K. Takamatsu, Phytosphingosine-containing neutral glycosphingolipids and sulfatides in the human female genital tract: their association in the cervical epithelium and the uterine endometrium and their dissociation in the mucosa of fallopian tube with the menstrual cycle, Keio J. Med. 41 (1992) 161–167.
[60] B. Roder, J. Dabrowski, U. Dabrowski, H. Egge, J. Peter-Katalinic, G. Schwarzmann, K. Sandhoff, The determination of phytosphingosine-containing globotriaosylceramide from human kidney in the presence of lactosylceramide, Chem. Phys. Lipids 53 (1990) 85–89.
[61] M.W. Crossman, C.B. Hirschberg, Biosynthesis of phytosphingosine by the rat, J. Biol. Chem. 252 (1977) 5815–5819.
[62] P. Urbina, M.I. Collado, A. Alonso, F.M. Goñi, M. Flores-Díaz, A. Alape-Girón, J.-M. Ruysschaert, M.F. Lensink, Unexpected wide substrate specificity of *C. perfringens* α-toxin phospholipase, Biochim. Biophys. Acta 1808 (2011) 2618–2627.